Journal of Integrative Agriculture 2016, 15(8): 1874–1882

Available online at www.sciencedirect.com

ScienceDirect

RESEARCH ARTICLE

Water and salt movement in different soil textures under various negative irrigating pressures

WANG Jia-jia[1, 2], HUANG Yuan-fang[1], LONG Huai-yu[2]

[1] *Department of Soil and Water Sciences, College of Resources and Environmental Sciences, China Agricultural University/ Key Laboratory of Arable Land Conservation (North China), Minstry of Agriculture/Key Laboratory of Agricultural Land Quality Monitoring, Ministry of Land and Resources, Beijing 100093, P.R.China*

[2] *Institute of Agricultural Resources and Regional Planning, Chinese Academy of Agricultural Sciences, Beijing 100081, P.R.China*

Abstract

This study examined the effect of different negative pressures and soil textures on water and salt movement to improve the efficiency of negative pressure irrigation (NPI). Four soil textures of varying fineness (Loamy Sand, Loam, Silty Loam, and Sandy Loam) and three negative pressure values (0, –5, and –10 kPa) were used. As irrigation time increased, wetting front movement speeds decreased, and as negative pressure increased, wetting front size decreased. Coarse soils had the smallest wetting front under greater negative pressure. Next, water infiltration rate decreased as irrigation time increased, and coarse soils had the lowest average infiltration rate under greater negative pressure. Finally, salt content increased with distance from the irrigation emitter and with increased negative pressure. Further, coarse soils were found to have decreased desalination under greater negative pressure. Thus, soil texture has a strong effect on NPI efficiency. However, by adjusting pressure values in accordance with soil texture, soil water content can be controlled and maintained. These findings are important to the improvement of NPI systems, increasing their practicality for agricultural use.

Keywords: negative pressure irrigation, volumetric water content, soil salt content, soil texture

1. Introduction

Chinese agricultural water consumption is 400 billion m^3 every year, which accounts for 65% of the nation's total water consumption (MWRPRC 2013). Irrigation accounts for more than 90% of the nation's total agricultural water consumption. Due to these extensive irrigation needs, China's effective irrigation water use (0.5), the ratio of irrigated water used by crops to total irrigated water, currently lags behind that of developed nations (0.7–0.8) (Hu 2013). It is therefore of great importance to increase water use efficiency through the improvement of existing irrigation methods. One such technique that has received recent attention is negative pressure irrigation (NPI), which relies on soil matrix suction to irrigate crops. By altering negative pressure, NPI controls water distribution based on the soil texture around crop roots during the entire growth period. NPI is a high-efficiency method that improves crop quality and increases water savings (Nalliah and Ranjan 2010). First, it can potentially be tailored to specific field conditions, and the second, the roots

Received 24 June, 2015 Accepted 19 October, 2015
WANG Jia-jia, E-mail: jiajia19202080@163.com;
Correspondence LONG Huai-yu, Tel: +86-10-82108776,
E-mail: hylong@caas.ac.cn

doi: 10.1016/S2095-3119(15)61209-6

are watered *via* capillary action, making it a system that is entirely controlled by plant water demand.

Studies on negative pressure irrigation methods have been performed since the early 20th century (e.g., Livingston 1918) and is now being successfully used in greenhouse production. For example, Wang *et al*. (2007) suggested that a soil matric potential of –25 kPa was the most favorable setting for potato (*Solanum tuberosum*) production, resulting in better crop performance than other treatments, as measured by a host of quality-related variables (e.g., height, tuber bulk rate and grade, water use efficiency, and irrigation water use efficiency). Further, hot peppers (*Capsicum annuum*: Nalliah *et al*. 2009, 2010) under –0.2 m capillary-irrigation performed better in terms of growth and yield parameters when compared with manual irrigation, while saving a substantial amount of water. The capillary-irrigation technique offers a precise water delivery with minimal labor, which is suitable for use in greenhouse pepper production and in areas where both water and workforce are scarce.

Given the promising outcomes of NPI, much research has focused on further improving NPI efficiency (Liu 2006) and the effects of this technique on crop growth. Among the variables of potential interest, previous studies have investigated evaporation rates, wetting body, wetting front, the cumulative amount of infiltration, and the maximum/minimum wetting distance over time (Jiang *et al*. 2004; Moniruzzaman *et al*. 2011a, b). However, relatively few studies have examined the effects of soil texture on NPI efficiency. The available research disagrees on what soil textures are most effective under NPI. For example, Xin (2007) found that more finely textured, cohesive soil results in poorer soil water infiltration. In contrast, Liang *et al*. (2011) found that cohesive soil performs better than less cohesive, sandy soil, as measured by greater cumulative water infiltration and the maximum wetting distance. Similar results were also reported by Jiang *et al*. (2005), comparing Sandy Loam to the more cohesive clay sand. These opposing conclusions may be a result of variation in irrigation equipment used by different research groups. Thus, for studies to draw reliable conclusions, it is necessary to control for the variation in equipment when investigating water movement under different soil textures.

In addition, previous research has shown that irrigation alters salt content in soil. For example, a favorable low salinity zone could be achieved around the roots when the soil matric potential threshold was kept under –25 kPa, at a depth of 20 cm below the drip irrigation emitter (Wang *et al*. 2011). This method greatly improved seed-cotton yield in the area, demonstrating that altering salt content *via* irrigation directly affects agricultural productivity. Next, Siyal *et al*. (2013) found that positive pressure in underground irrigation causes water movement to the surface *via* capillary action, and once this water evaporates, the resultant salt accumulation increases soil salinity to unacceptable levels. In contrast, the negative pressure methods could reduce capillary water content, decreasing both surface evaporation and deep percolation, resulting in more usable water around the root zone (Nalliah *et al*. 2009). Despite these findings, knowledge remains limited with regard to how NPI affects soil salt movement around the root zones of crops. Such information is especially critical for major salt-sensitive crops such as maize (Ding *et al*. 2012) and tomato (Hanson *et al*. 2009). Understanding both water and salt movement when using this irrigation method will be extremely beneficial to improving the design and management of NPI systems for different soil textures.

Thus, the objectives of this study were 1) to examine the effects of soil texture on soil water and salt movement around irrigation emitters in NPI, and 2) to examine how changes to negative pressure values affect water and salt movement within different soil textures, thereby providing a reliable basis for the future application of NPI technology.

2. Materials and methods

The study was conducted from May to September in 2014, at the Institute of Agricultural Resources and Regional Planning Laboratory, Chinese Academy of Agricultural Sciences, Beijing. The site is located at 116°19′18′′N, 39°57′40′′E, about 56 m above average sea level.

2.1. System design

The irrigation system consists of three parts: the negative pressure generator (the solenoid valve and mercury gauge are only used when the irrigation system is actually used for crops), water tank, and irrigation emitter (patented by the Chinese Academy of Agricultural Sciences; patent no. 200710178527.3). The latter consists of a 23-cm long porous ceramic pipe, with inner and outer diameters of 10 and 18 mm, respectively. This NPI system has been successfully used in growing flue-cured tobacco, improving various botanical traits compared with plants grown under other systems (Xiao *et al*. 2015).

The laboratory setup is illustrated in Fig. 1. The irrigation system is connected to a special soil bin (internal dimensions: 250 mm×20 mm×500 mm) made of 5-mm thick, clear polymethyl methacrylate. A polyvinyl chloride film was placed on the front of the soil bin to manually record wetting front boundaries. During the experiments, negative pressure was solely controlled by the height (h) between the irrigation emitter and the air contact point, which yields the most accurate negative pressure (Fig. 1). Prior to the start of every experiment, any water in the intake tube was

drained. The air contact point, therefore, was always at the bottom of the intake tube when the experiment began.

During irrigation, water levels decrease in the tank and water pressure correspondingly decreases. However, air then enters the water tank through the intake tube, balancing the pressure in the water tank with atmospheric pressure. In sum, the supply water pressure in the irrigation emitter is:

$$P=P_0-\rho gh \quad (1)$$

Where, P, supply water pressure in irrigation emitter; P_0, atmospheric pressure; h, water column height between irrigation emitter and air contact point; g, 9.8 N kg^{-1}; ρ, water density. The negative pressure between the intake tube and the irrigation emitter is –ρgh.

The irrigation system activates when the ceramic irrigation emitter is placed into dry soil. Irrigation water from the filled tank then encounters the low levels of soil water through micro-pores in the emitter. Crop roots proceed to absorb irrigated water from the soil, lowering soil water potential. This results in water movement from high potential (in the irrigation container) to low potential (in soil) through the NPI emitter. Irrigation is terminated when the soil water potential is higher than the water potential, and resumes once sufficient crop root water uptake occurs to lower soil water potential again.

2.2. Experimental methods

Four soils were used in the experiments, each with a different texture: Loamy Sand (LS), Loam (L), Silty Loam (SL), and Sandy Loam (SL). Table 1 shows the basic physical properties of each soil texture and their corresponding codes, by which the soil textures will be hereafter referred. Fig. 2 shows the measured soil water retention curve of the four soils.

To achieve an equal balance of salt across all soil textures, 10 g kg^{-1} NaCl was dissolved in distilled water for each soil texture and mixed with the soils. After leaving overnight, the salt-soil mixture was crushed, weighed, air dried, and sieved (in a 2-mm sieve). Soils were loaded and compacted into the soil bin in 2.5 cm layer to obtain the most homogeneous soil profile possible. Bulk density of the soils was 1.4 g cm^{-3}. The saturated hydraulic conductivity of the irrigation emitter was 0.46 cm d^{-1}, measured using the constant head method (Siyal *et al*. 2009a). During soil packing, the irrigation emitter was placed approximately 20 cm from the soil surface. Altering h by lifting or lowering the

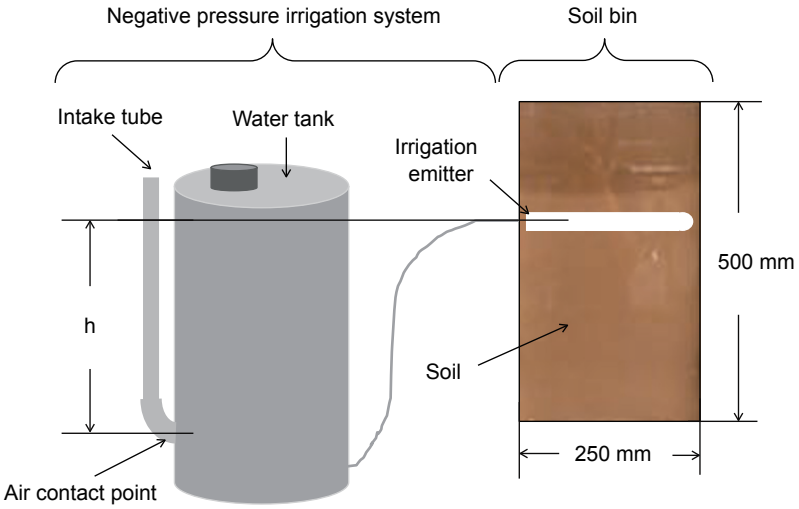

Fig. 1 A schematic diagram of the experimental design.

Table 1 Basic physical properties of experimental soils

Soil texture	Soil mechanical composition (%)[1)]			EC[2)] (dS m^{-1})	K_s[3)] (10^{-6} cm s^{-1})
	Sand (≥0.05 mm)	Silt (0.05–0.002 mm)	Clay (≤0.002 mm)		
Loamy Sand (LS)	88.46	1.15	10.39	3.17	8.28
Sandy Loam (SL)	59.48	32.60	7.92	3.74	2.06
Loam (L)	49.31	29.38	21.31	3.76	3.02
Silty Loam (SiL)	31.04	50.39	18.56	3.79	1.46

[1)] Values in brackets refer to soil particle size.
[2)] EC is the electrical conductivity (EC1:5; dS m^{-1}) of soil:water (1:5, w:v) extracts.
[3)] K_s is saturated hydraulic conductivity.

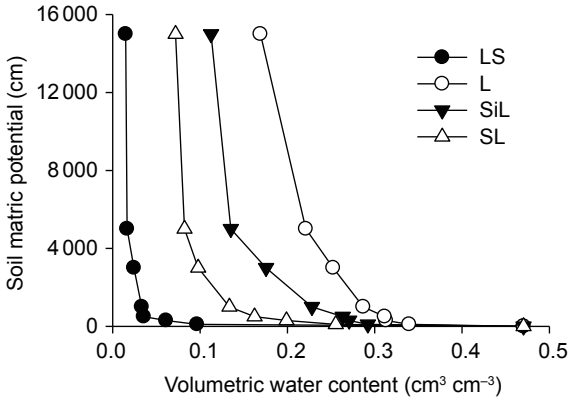

Fig. 2 Soil water retention curve of LS (Loamy Sand), L (Loam), SiL (Silty Loam), and SL (Sandy Loam).

soil bin resulted in the negative pressure required (Fig. 1). The study was carried out for three different negative pressures: 0, –5 and –10 kPa, corresponding to h=0, 51 and 102 cm, respectively.

Wetting front positions and the amount of water infiltration were recorded from t=1–8 h. To mark wetting front positions, a line was directly drawn with a marker on the polyvinyl chloride film in front of the soil bin. After 8 h, the total amount of water infiltration was recorded at t=24 h. Samples of 1-cm thickness above and below the pipe emitter were also obtained, to determine the volumetric water content and the electrical conductivity (EC1:5; dS m^{-1}) of the soil:water (1:5, w:v) extracts, which was obtained after treating soil samples with a leaching solution. Volumetric water content was calculated using the oven-drying method. EC was measured using a conductivity meter (DDS-307 Co., China). Detailed methods were previously described by Bao (2000).

2.3. Data analysis

Wetting front data collection was performed using the GetData Graph Digitizer software (ver. 2.26; Fedorov 2013). All statistical analyses were performed using SigmaPlot 12.5 (Systat Software Inc., San Jose, CA).

3. Results

3.1. Wetting front dynamics of different soil textures under various irrigation pressures

The wetting front is an index that characterizes soil water movement. Fig. 3 shows the wetting fronts at t=1–8 h for different soil and negative pressure ($|P_n|$) treatments. The wetted zone of different soil textures decreased as the $|P_n|$ increased. Movement speed of the wetting front was faster at the beginning of the experiment, but slowed as irrigation time increased. Across all treatments, the downward wetting front was faster than the upward wetting front, due to gravity.

The greatest distance between the upward (h_u) and downward (h_d) wetting front to the irrigation emitter occurred at t=8 h and P_n=0 kPa for all four soil textures, with the exception of SL soil, where the greatest distance occurred at P_n=–5 kPa (Table 2). Specifically, for LS soil, h_u=13.5 cm and h_d=28.5 cm. For L soil, h_u=5.9 cm and h_d=8.6 cm. For SiL soil, h_u=4.9 cm and h_d=5.2 cm. Finally, for SL soil, h_u=3.7 cm and h_d=4.8 cm. It should also be noted that h_u and h_d for SL soil at P_n=0 kPa did not significantly differ from P_n=–5 kPa; they were h_u=4.3 cm and h_d=4.7 cm.

At higher negative pressure, (i.e., P_n = –5 and –10 kPa), the condition was reversed, with SL soil having the largest wetted zone, followed by L and SiL soils, then by LS soil with the smallest wetted zone.

3.2. Water infiltration rate change of different textural soils under various irrigation pressures

Water infiltration rate reflects the amount of water that enters the soil per unit time. Fig. 4 shows the water infiltration rates at t=1–8 h for different soil and negative pressure conditions. Water infiltration rate clearly decreased as suction increased, across all soil textures. Subsequent values are all from t=8 h. At P_n=0 kPa, average water infiltration rates of LS, L, SiL, and SL soils were 9.2, 5.0, 1.8, and 1.2 mm h^{-1}, respectively. At P_n=–5 kPa, average water infiltration rates of LS, L, SiL, and SL soils were 0.4, 1.6, 0.8, and 1.3 mm h^{-1}, respectively. Lastly, at P_n=–10 kPa, average water infiltration rates of LS, L, SiL, and SL were 0.1, 1.1, 0.7, and 0.7 mm h^{-1}, respectively.

Under P_n=0 kPa, the water infiltration rate of L soil was greater than LS at t=1, but LS soil water infiltration rate far exceeded L (and all other soils) after 2 h. In contrast, water infiltration rates at P_n=–5 and –10 kPa were L>SL>SiL>LS. The change in P_n thus produced an effect on LS water infiltration rates that was greater than the effect on other soils.

3.3. Soil moisture distribution of different textural soils under various irrigation pressures

Volumetric water content decreased overall with increasing $|P_n|$ at t=24 h (Fig. 5). The same inverse trend of volumetric water content and distance from the emitter occurred across different soil and negative pressure treatments. Specifically, volumetric water content was the highest around the emitter and gradually decreased as distance from the emitter increased. At P_n=0 kPa, volumetric water content of LS

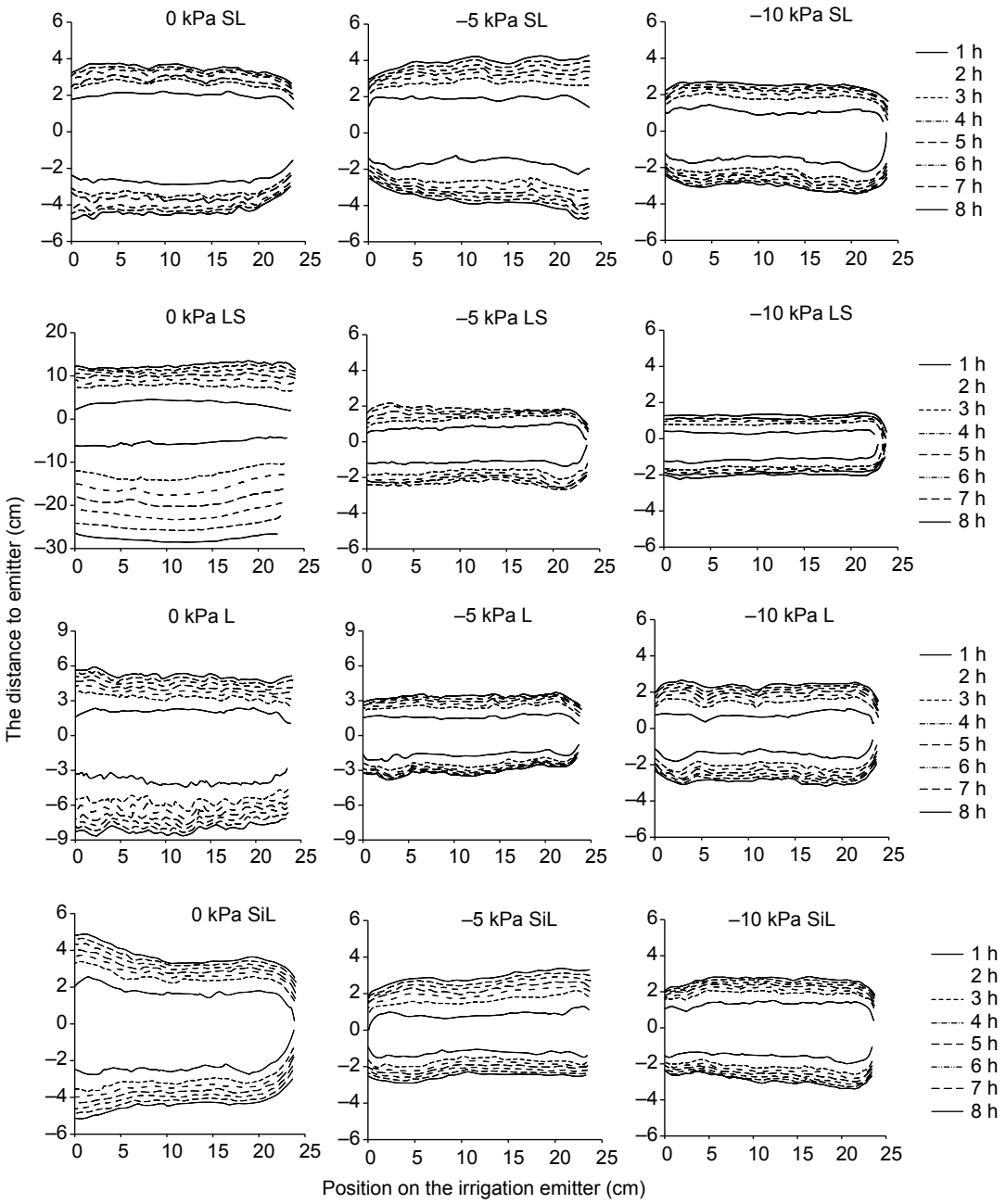

Fig. 3 Wetting front dynamics over time of four soil textures under three irrigation pressures. On the *Y* axis, 0 represents the centre of the irrigation emitter; thus, positive and negative values represent position of soil above and below the irrigation emitter, respectively; 0, –5 and –10 kPa represent different irrigation pressure settings. The same as below.

remained relatively uniform above 6.0 cm and below 18.0 cm from the emitter.

Average volumetric water content of the four soils was L>SiL>SL>LS across all three negative pressures. Within each soil texture, increasing the negative pressure (0 to –5 to –10 kPa) decreased volumetric water content. Although the decreasing trend was the same, the four soils varied in the amount of water they could retain, depending on the negative pressure.

3.4. Total amount of water infiltration of different soil textures under various irrigation pressures

The water infiltration data are shown in Fig. 6. Total water infiltration was the greatest at P_n=0 kPa for all soil textures. Both LS and L soils exhibited very high (and similar) water infiltration at zero pressure. However, with increased negative pressure, LS soil water infiltration plummeted by 93.5–96.2%. Other soil textures also experienced large

Table 2 Distance between upward (h_u) and downward (h_d) wetting front to the irrigation emitter at t=8 h for all four soil textures and at three irrigation pressures

Irrigation pressure (kPa)	LS (cm)		L (cm)		SiL (cm)		SL (cm)	
	h_u	h_d	h_u	h_d	h_u	h_d	h_u	h_d
0	13.5	28.5	5.9	8.6	4.9	5.2	3.7	4.8
–5	2.4	3.0	3.7	3.8	3.4	2.9	4.3	4.7
–10	1.4	2.2	2.7	3.2	2.9	3.4	2.7	3.4

drops in water infiltration levels at higher negative pressures, but none as dramatically as LS soil. Specifically, L soil declined by 70.4–78.0%, SL soil declined by 24.5–55.5%, and SiL declined by 5.9–55.9%. Thus, at P_n=–5 and –10 kPa, water infiltration across the soils was L>SL>SiL>LS.

3.5. Soil salinity distribution of different soil textures under various irrigation pressures

Fig. 7 shows a positive correlation between EC values and distance from the emitter; EC increased with distance from the emitter increased, a trend observed across all soil and pressure treatments. This corresponds to salt concentrations, which was the lowest around the emitter and higher with increasing distance from the emitter. At the same time, as $|P_n|$ increased, salt accumulated in the wetting front and desalted regions decreased.

At P_n=0 kPa, the pressure setting with the highest desalination, average EC in the desalted regions was LS<L<SiL<SL. This corresponds to the size of the desalted regions, which was approximately (–21.0)–7.0 cm for LS soil, (–7.0)–5.0 cm for L soil, (–5.0)–4.0 cm for SiL soil, and (–4.0)–3.0 cm for SL soil. LS soil saw the greatest reduction in salt compared to the start of the experiment, with a decrease of 91.8%. L and SiL soils were desalinated by 81.1 and 80.2%, SL soil was desalinated by 65.8%.

At P_n=–5 kPa, average EC was SiL<SL<L<LS. The desalted regions of all soil textures decreased, with LS soil dropping the most drastically to approximately (–2.0)–1.0 cm, while the other three soils had desalted regions of approximately (–3.0)–3.0 cm. Desalination still occurred at this negative pressure value, although at lower levels than zero pressure. SiL soil was desalinated by 70.7%, SL soil by 66.0%, L soil by 61.4%, and LS soil by 33.4%.

Finally, at P_n=–10 kPa, average EC was SiL<SL<L<LS. Desalted regions were the smallest at this pressure value; L and SiL soils were approximately –2.0 to 2.0 cm, while LS and SL soils were –1.0 to 1.0 cm. Compared to the start of the experiment, SiL soil was desalinated by 57.0%, SL and

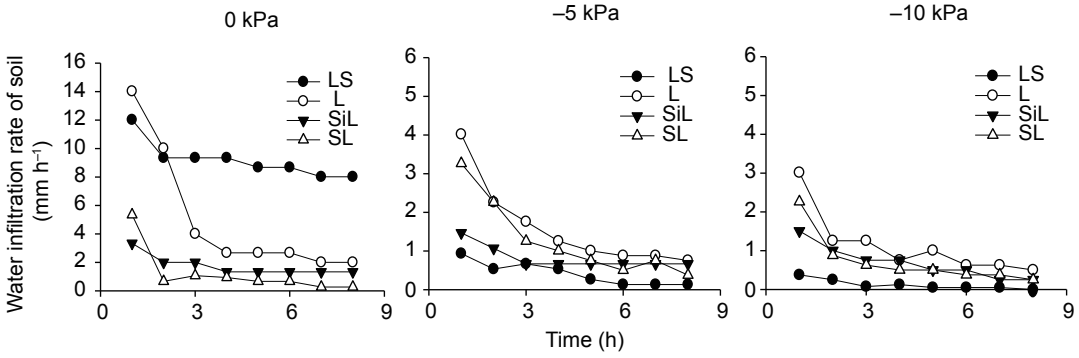

Fig. 4 Change in water infiltration rates of four soil textures under three irrigation pressures.

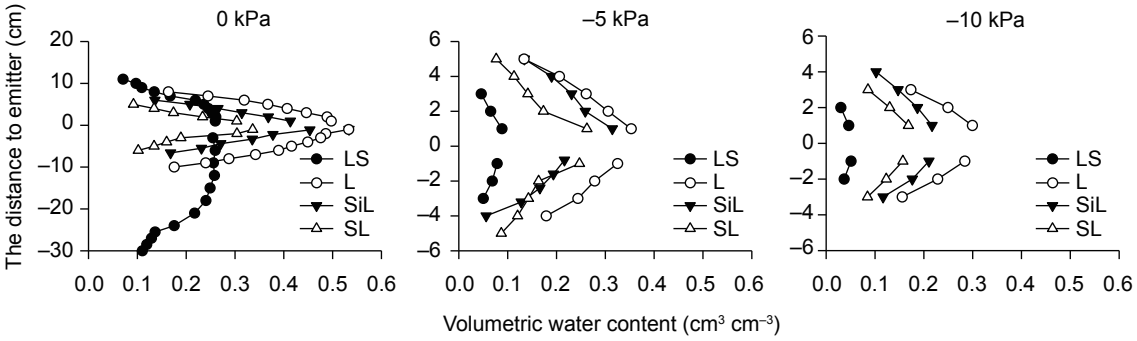

Fig. 5 Soil moisture distribution of four soil textures under three irrigation pressures.

L soils were desalinated by 52.9 and 49.2% respectively, and LS soil was desalinated by 33.4%.

4. Discussion

This study investigated the effects of varying soil texture and negative pressure on the efficiency of NPI. Specifically, at the same soil matric potential (Fig. 2), finer soil (L) had the highest volumetric water content and coarse soil (LS) had the lowest, indicating that soil infiltration characteristics were poorest in soils with the largest particles. This outcome corroborates with previous research (Jiang *et al*. 2005; Liang *et al*. 2011), and can be explained by the small pores and low matric potential of fine-grained material, which results in increased suction of water into the soil. Moreover, by comparing different soil textures in one study, we avoided potential errors that may result from differences in methods, lending stronger support to our experimental outcome.

Although saturated hydraulic conductivity is the greatest in LS, implying that coarse soil should irrigate water well, the large particles in LS result in bigger gaps between particles (Jiang *et al*. 2005; Liang *et al*. 2011), which is a key factor in NPI effectiveness. To elaborate, a dramatic difference was observed between the wetted zones of LS at zero *vs*. increasingly negative pressures. At zero pressure, the saturated hydraulic conductivity (K_s) is the highest for LS. However, at high negative pressures, K_s drops, and capillary action is weak in the large pores between LS soil particles. Therefore, the soil matrix suction of LS is correspondingly low, in comparison to other soils at the same volumetric water content, and it is unable to absorb irrigation water. In contrast, soils with finer textures (smaller particles) have larger surface area, which results in greater soil matrix suction and therefore higher degrees of water infiltration when irrigated.

Interestingly, the results reported here are at odds with another study that found soils with smaller particles to have worse water infiltration under negative pressure irrigation, compared with soils with larger particles (Xin 2007). A methodological difference may account for these contradicting outcomes. Specifically, Xin (2007) used gauze as the irrigation emitter rather than the porous pipe used in this study. The greater permeability of gauze could have resulted in more air moving into the water tank, altering the negative pressure to zero, or even positive pressure. As already stated, soils with large particles have high hydraulic conductivity at zero pressure, and a previous study revealed that the wetted zone and emission rate are larger in coarse soil than in fine soils under positive pressure (Ashrafi *et al*. 2002; Gupta *et al*. 2009; Siyal *et al*. 2009a, b). These two factors explain why Xin (2007) saw results in opposition to those reported in this study.

While all four soil textures held less water as negative pressure increased, there was significant variation in the water content both within and across each soil texture, in response to changes in negative pressure. These findings are in line with other studies investigating the effects of pressure on soil water content. For example, Zhao (2011) reported that clay loam moisture decreases with a negative

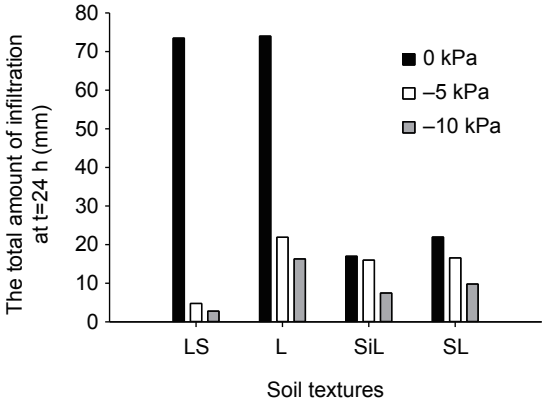

Fig. 6 Total amount of water infiltration of four soil textures under three irrigation pressures at t=24 h.

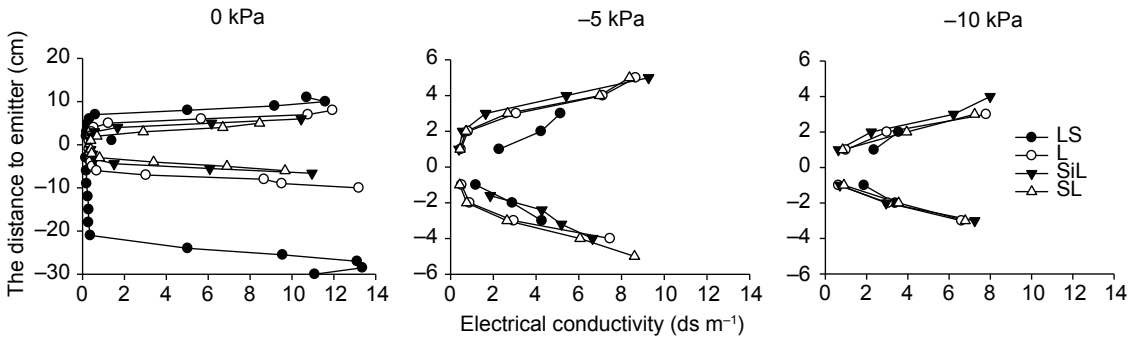

Fig. 7 Electrical conductivity (EC1:5) distribution of four soil textures under three irrigation pressures at t=24 h.

pressure increase, and the same pattern was found in the coarser Kawanishi sand (Moniruzzaman *et al*. 2011a). However, the change in water content was much greater in finer soil (0.32–0.19 cm^3 cm^{-3}, Zhao 2011) compared with coarser soil (0.14–0.11 cm^3 cm^{-3}, Moniruzzaman *et al*. 2011a). Moreover, under negative pressure irrigation (P_n=–10 kPa), the water content of the finer-grained clay and clay loam reached 0.39 cm^3 cm^{-3} (Lipiec *et al*. 1998) and 0.47 cm^3 cm^{-3} (Iwama *et al*. 1991), respectively. These studies, in combination with the results reported herein, indicate that while volumetric water content in soils can be controlled by setting different negative pressures in NPI, such adjustments must be tailored to the specific soil texture. Furthermore, the similar patterns across different locations suggest that our results are broadly applicable to soils around the world.

Finally, NPI is effective in leaching salt from soil located near the emitter, creating a desalted region around that area. Thus, salt accumulation only occurs in the wetting front away from this desalted region. Furthermore, higher negative pressure was less effective than zero pressure irrigation at desalinating the soil. However, the size of the desalted region and the amount of salt reduced was highly dependent on differences in soil texture. In turn, patterns of desalination were closely related to water movement patterns in these different soils.

Thus, future applications of NPI in agricultural practices should take into account both differences in irrigation pressure and the texture of the target soil. For example, while potato has the highest production in L soil under a soil matric potential of –25 kPa (Wang *et al*. 2007), we can potentially achieve the same productivity in SL by altering the irrigation pressure, so that the same soil moisture is achieved. Similarly, because crop roots are extremely active in absorbing water at the soil and emitter interface (Abidin *et al*. 2014), we can adjust negative pressure to controlling soil water and salt levels around the emitter, thereby improving the growing environment of the roots. Such techniques should vastly improve irrigation quality and therefore, increase crop quality and yield.

5. Conclusion

Soil texture significantly affects soil salt and water distribution when using a negative pressure irrigation system. As negative pressure increases in NPI, the degree of salt leaching and soil water infiltration (as measured by water infiltration rate, wetted zone, volumetric water content, and total amount of water infiltration) both decrease. Specifically, at the same negative pressure, L soil exhibited the fastest water infiltration and the highest soil moisture (0.23–0.25 cm^3 cm^{-3}), followed by SiL (0.17–0.19 cm^3 cm^{-3}), SL (0.13–0.15 cm^3 cm^{-3}), and finally, LS (0.04–0.07cm^3 cm^{-3}), which also had the slowest water infiltration rates. Adjusting negative pressure values in accordance to soil texture can therefore maintain a certain level of soil water content. Under NPI, desalination was the highest in SiL (57.0–70.7%), moderate in L and SL, and the lowest in LS (33.4%). These patterns demonstrate that soils with larger particles have poorer soil water infiltration and experience decreased desalination, compared with fine soils. Notably, under zero pressure irrigation, this pattern was reversed, with finer soils experiencing decreased desalintion.

In summary, this study demonstrates the need to include soil texture as a variable when applying negative pressure irrigation systems for practical agricultural use. Differences in soil texture will greatly affect irrigation efficiency.

Acknowledgements

This project was supported by the National High-Tech R&D Program of China (2013AA102901). The authors thank Cong Ping, Jiang Yuzhou, Wang Xiangling, and Xiao Haiqiang who are members of a research group studying “Technology for Crop Growth Moisture and Nutrient Soil Habitat Control”, they provided great help in my life and the test. We also thank the Institute of Agricultural Resources and Regional Planning of Chinese Academy of Agricultural Sciences for providing the negative pressure irrigation device.

References

Abidin M S B Z, Shibusawa S, Ohaba M, Li Q, Khalid M B. 2014. Capillary flow responses in a soil-plant system for modified subsurface precision irrigation. *Precision Agriculture*, **15**, 17–30.

Ashrafi S, Gupta A D, Babel M S, Izumi N, Loof R. 2002. Simulation of infiltration from porous clay pipe in subsurface irrigation. *Hydrological Sciences Journal*, **47**, 253–268.

Bao S D. 2000. *Soil Agricultural Chemistry Analysis*. China Agriculture Press, Beijing, China. (in Chinese)

Ding D, Xiao Z X, Xiao H L, Xia T, Zheng Y L, Qiu F Z. 2012. Revelation of the early responses of salt tolerance in maize *via* SSH libraries. *Genes & Genomics*, **34**, 265–273.

Fedorov S. 2013. GetData graph digitizer. [2014-06-01]. http://getdata-graph-digitizer.com

Gupta A D, Babel S M, Ashrafi S. 2009. Effect of soil texture on the emission characteristics of porous clay pipe for subsurface irrigation. *Irrigation Science*, **27**, 201–208.

Hanson B R, May D M, Simunek J, Hopmans J W, Hutmacher R B. 2009. Drip irrigation provides the salinity control needed for profitable irrigation of tomatoes in the San Joaquin Valley. *California Agriculture*, **63**, 131–136.

Hu S Y. 2013. Opinion of the state council on strict water management system: Background and main contents of press conference. [2013-04-22]. http://www.xinhuanet.com/zhibo/20120216/zx.htm

Iwama H, Kubota T, Ushiroda T, Osozawa S, Katou H. 1991. Control of soil water potential using negative pressure water circulation technique. *Soil Science Plant Nutrition*, **37**, 7–14.

Jiang P F, Lei T W, Bralts V F, Liu H. 2005. The interactive effects of emitters and soil textures on soil water movement under the negatively pressurized irrigation system. *ASAE Annual International Conference*. American Society of Agricultural and Biological Engineers, Joseph, MI. p. 052250.

Jiang P F, Lei T, Xiao J, Yu Y, Bralts V F. 2004. A new irrigation system of zero/negative pressure and the experimental verification of its feasibility. *ASAE/CSAE Annual International Conference*. American Society of Agricultural and Biological Engineers, Joseph, MI. p. 042253.

Liang J T, Sun X H, Xiao J. 2011. Influence of soil texture and water-supply head on soil water transportation under negative pressure irrigation. *Water Saving Irrigation*, **6**, 30–33. (in Chinese)

Lipiec J, Kubota T, Iwama H, Hirose J. 1998. Measurement of plant water use under controlled soil moisture conditions by the negative pressure water circulation technique. *Soil Science Plant Nutrition*, **34**, 417–428.

Liu M, Kojima T, Tanaka M. 2006. Development of soil-cooling and auto-irrigating system with negative pressure. *Transactions of the ASABE*, **49**, 239–244.

Livingston B E. 1918. Porous clay cones for the auto-irrigation of potted plant. *Plant World*, **11**, 39–40.

Moniruzzaman S M, Fukuhara T, Ito M, Ishii Y. 2011a. Seepage flow dynamics in a negative pressure difference irrigation system. *Journal of Japan Society of Civil Engineer* (Ser. B1), **67**, 97–102.

Moniruzzaman S M, Fukuhara T, Terasaki H. 2011b. Experimental study on water balance in a negative pressure difference irrigation system. *Journal of Japan Society of Civil Engineer* (Ser. B1), **67**, 103–108.

MWRPRC (Ministry of Water Resources of the People's Republic of China). 2013. China water resources bulletin. [2012-12-01]. http://www.mwr.gov.cn/zwzc/hygb/szygb/qgszygb/201411/t20141120_582980.html

Nalliah V, Ranjan R S. 2010. Evaluation of a capillary-irrigation system for better yield and quality of hot pepper (*Capsicum annuum*). *Applied Engineering in Agriculture*, **26**, 807–816.

Nalliah V, Ranjan R S, Kahimba F C. 2009. Evaluation of a plant-controlled subsurface drip irrigation system. *Biosystems Engineering*, **102**, 313–320.

Siyal A A, Martinus T, Genuchten V, Skaggs T H. 2009a. Performance of pitcher irrigation system. *Soil Science*, **174**, 312–320.

Siyal A A, Martinus T, Genuchten V, Skaggs T H. 2013. Solute transport in a loamy soil under subsurface porous clay pipe irrigation. *Agricultural Water Management*, **121**, 73–80.

Siyal A A, Skaggs T H. 2009b. Measured and simulated soil wetting patterns under porous clay pipe sub-surface irrigation. *Agricultural Water Management*, **96**, 893–904.

Wang F X, Kang Y H, Liu S P, Hou X Y. 2007. Effects of soil matric potential on potato growth under drip irrigation in the North China Plain. *Agricultural Water Management*, **88**, 34–42.

Wang R S, Kang Y H, Wan S Q, Hu W, Liu S P, Liu S H. 2011. Salt distribution and the growth of cotton under different drip irrigation regimes in a saline area. *Agricultural Water Management*, **100**, 58–69.

Xin C. 2007. Studies on the characteristics of soil water movement and determination of hydraulic parameters under negative hydraulic head. Ph D thesis, Xi'an University of Technology, Shanxi, China. (in Chinese)

Xiao H Q, Liu X Y, Long H Y, Yang H Q, Zhao B D, Guan E S, Wang D H, Yue X L. 2015. The effects of soil water potential on the growth and water consumption of flue-cured tobacco. *Chinese Tobacco Science*, **36**, 35–41. (in Chinese)

Zhao Y N. 2011. Effect of water head, emitter and water quality on soil water movements under negative pressure irrigation. Ph D thesis, Taiyuan University of Technology, China. (in Chinese)

(Managing editor WANG Ning)